[CII]輝線で探る銀河相互作用、インフロー、アウトフロー

1. Appleton+13 - 銀河相互作用
2. Brisbin+14 - インフロー（間接的）
3. Kreckel+14 -アウトフロー

[CII]158um微細構造輝線

- 11.3 eV photons to form C+
  - probe of the atomic gas heated by the FUV (6 - 13.6 eV) radiation field from massive stars
  - indicator of star formation rate
- 低励起(91 K above ground)
  - the dominant coolant of the neutral ISM
- optically thin
  - measure of the atomic gas mass

1. Appleton et al. 2013, ApJ, 777, 66

Shock-enhanced C^+ Emission and the Detection of H_2O from the Stephan's Quintet Group-wide Shock Using Herschel

銀河相互作用によるショック領域で[CII]が明るくなることがわかった

Stephan's Quintet

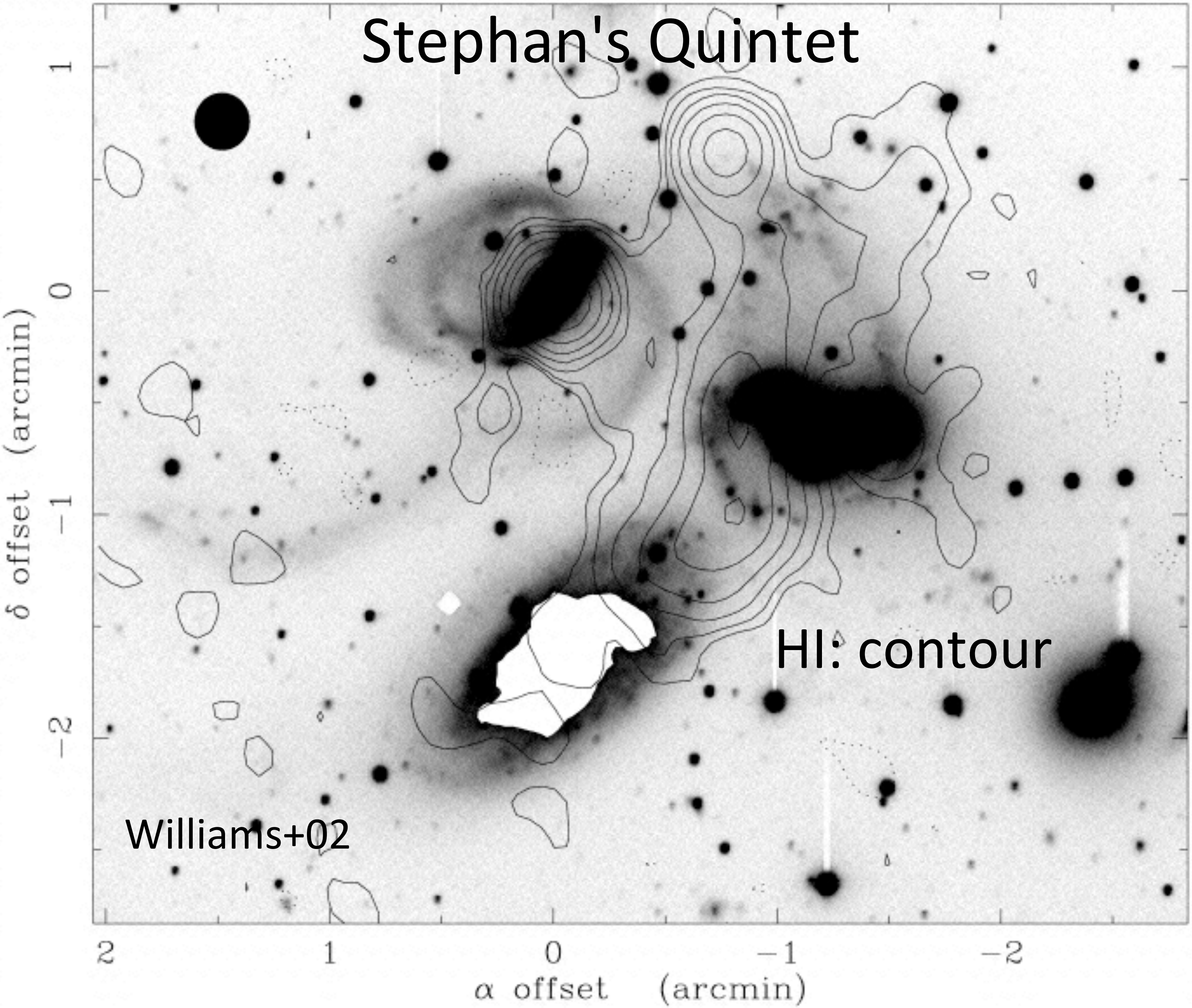

Stephan's Quintet

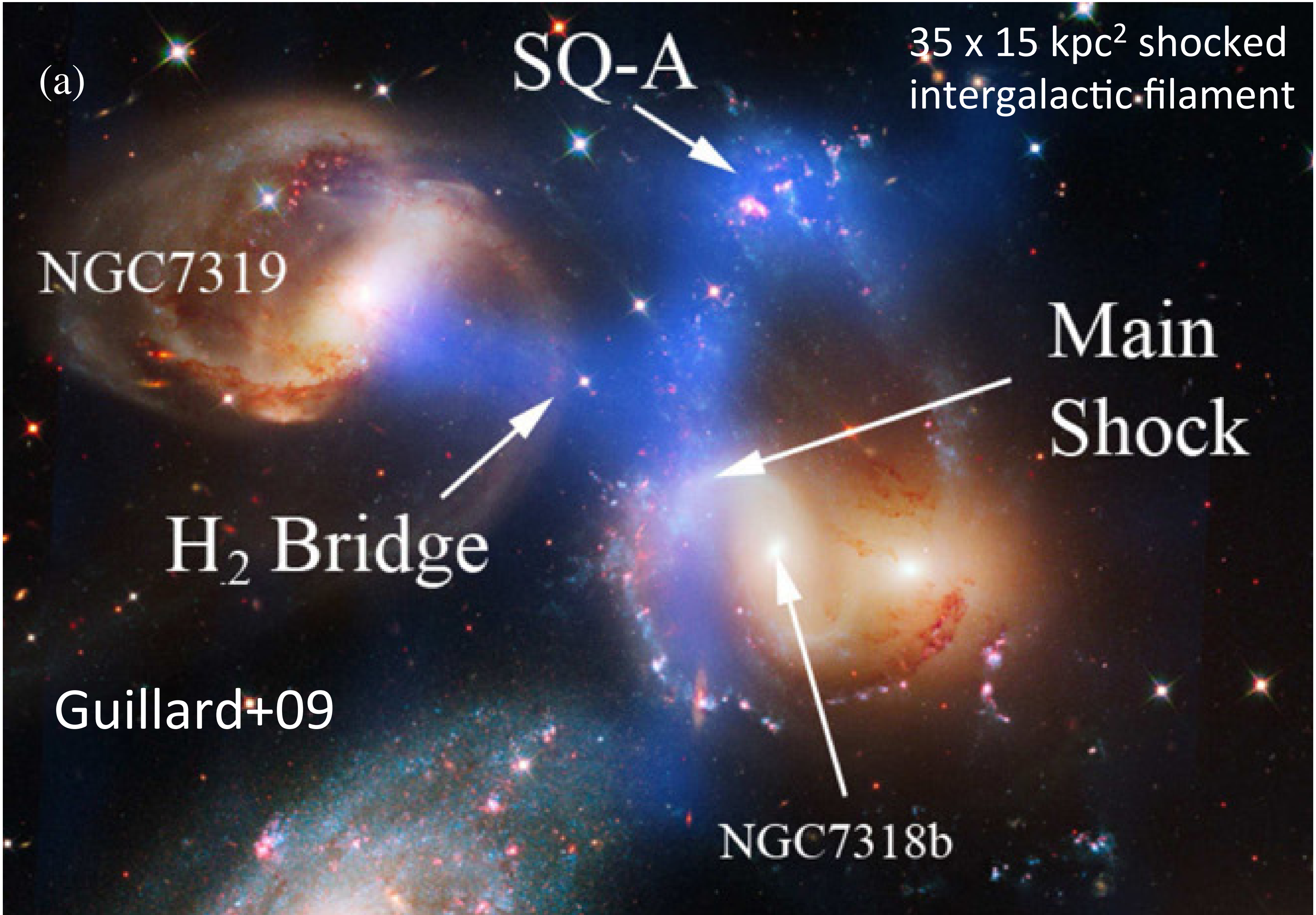

Stephan's Quintet

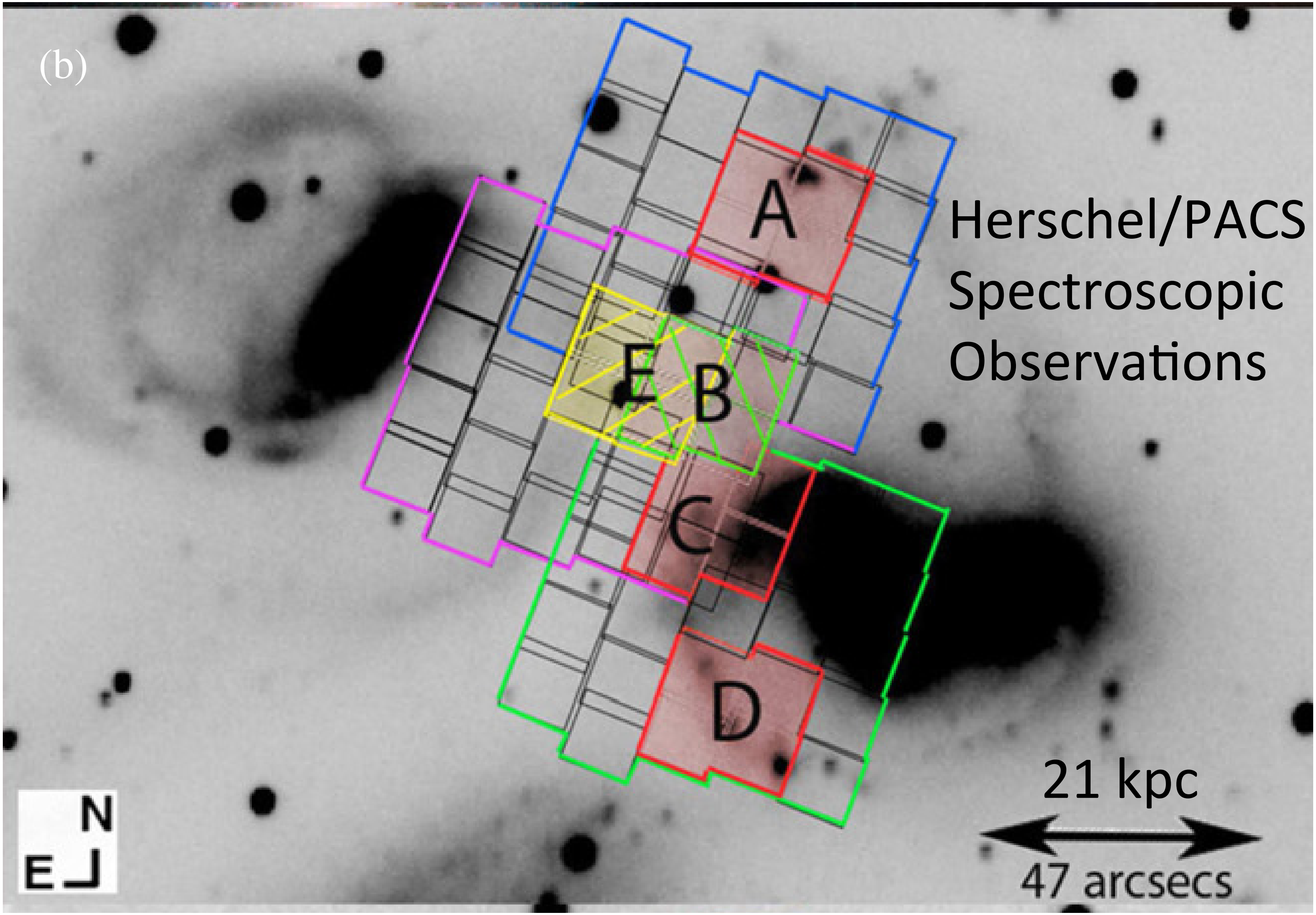

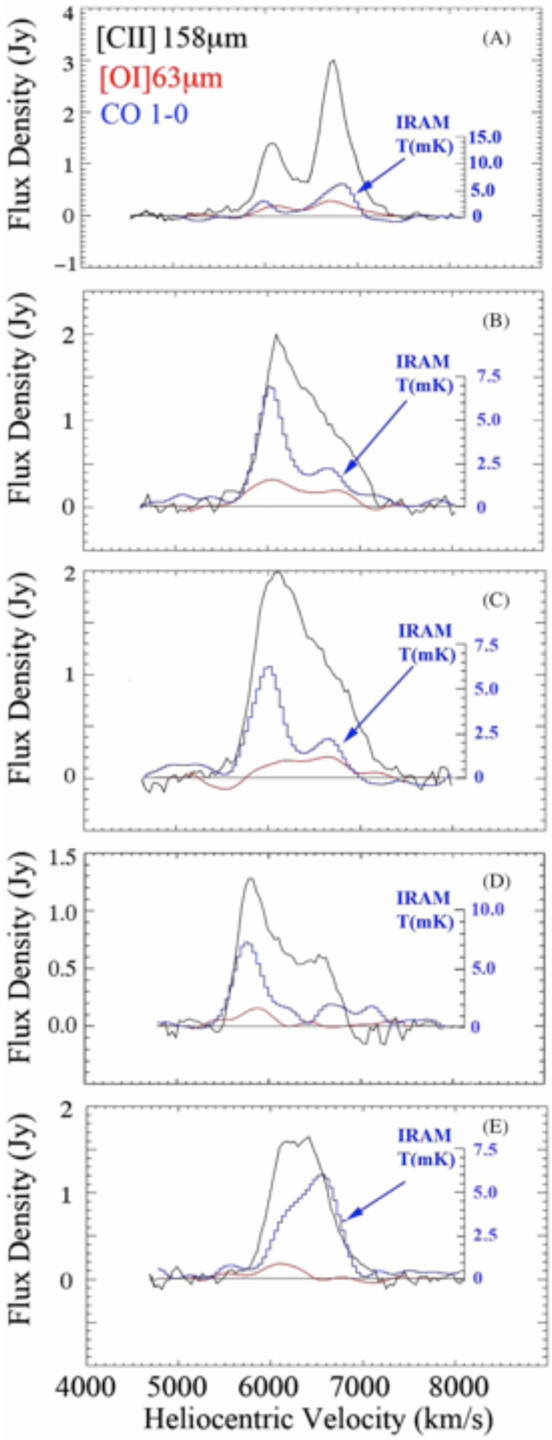
[CII] 158μm
[OI]63μm
CO 1-0
(A)
(B)
(C)
(D)
(E)
IRAM
T(mK)
Flux Density (Jy)
Heliocentric Velocity (km/s)
4000 5000 6000 7000 8000

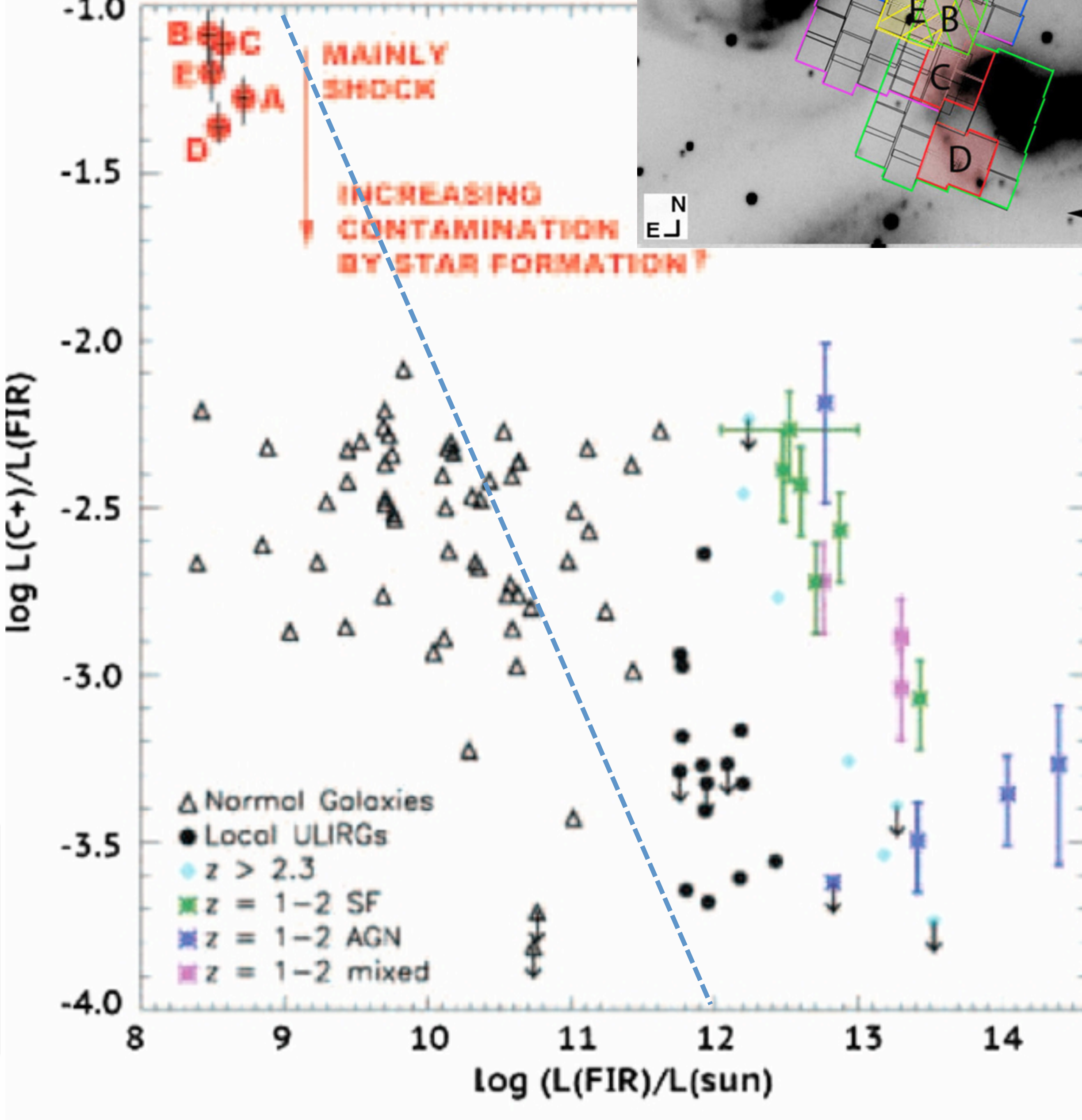
Log L(C+)/L(sun)=8
MAINLY SHOCK
INCREASING CONTAMINATION BY STAR FORMATION?
B
C
E
A
D
Normal Galaxies
Local ULIRGs
z > 2.3
z = 1–2 SF
z = 1–2 AGN
z = 1–2 mixed
log L(C+)/L(FIR)
log (L(FIR)/L(sun))
-1.0
-1.5
-2.0
-2.5
-3.0
-3.5
-4.0
8 9 10 11 12 13 14

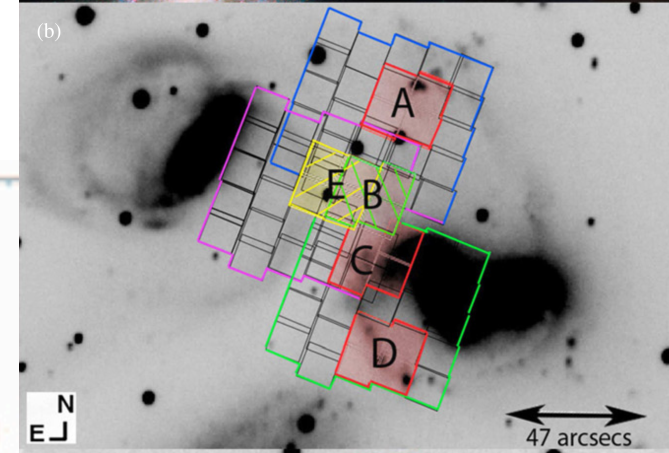
(b)
A
E
B
C
D
N
E
47 arcsecs

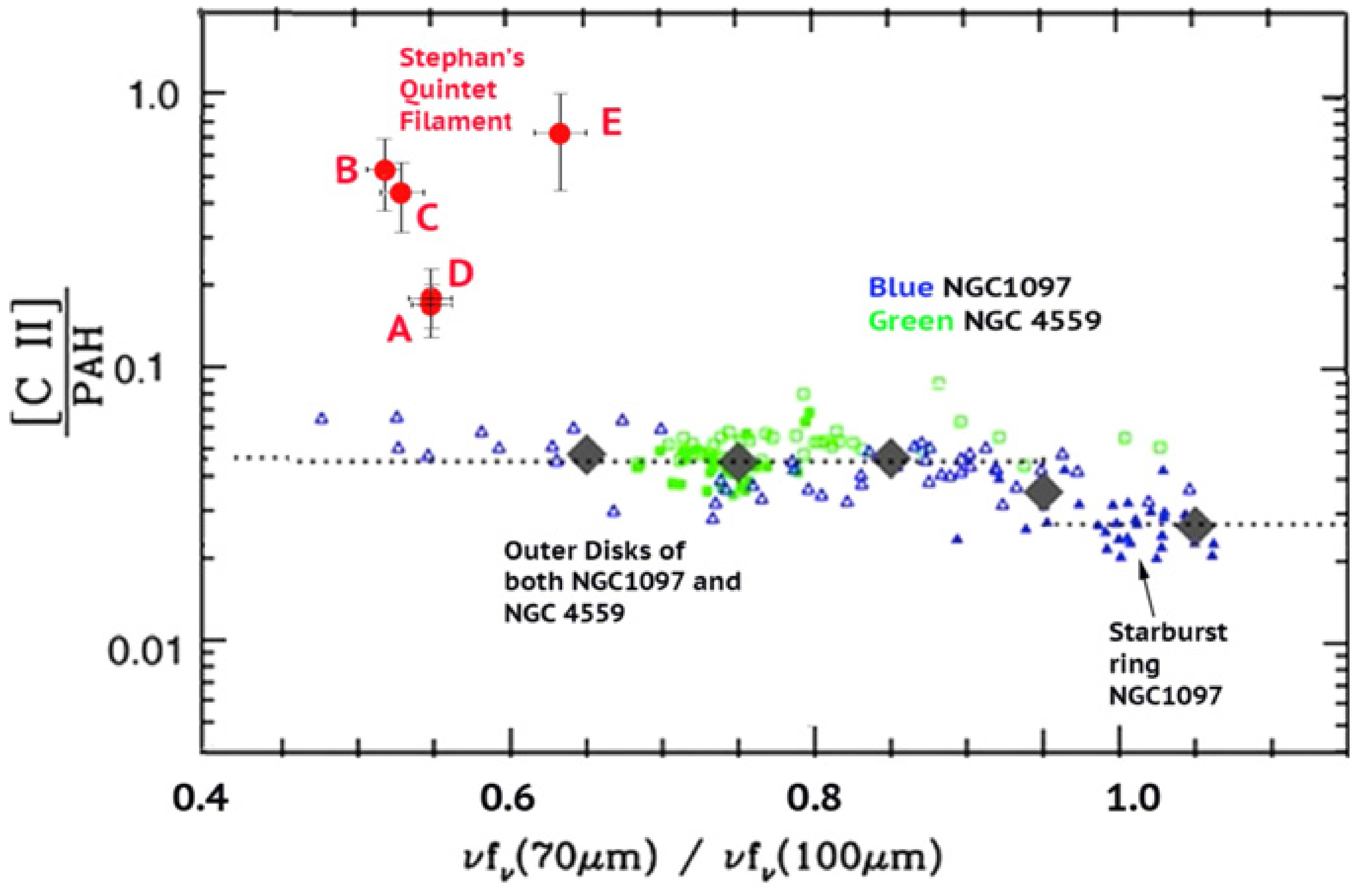

Stephan's
Quintet
Filament
A
B
C
D
E
Blue NGC1097
Green NGC 4559
Outer Disks of
both NGC1097 and
NGC 4559
Starburst
ring
NGC1097
1.0
0.1
0.01
0.4
0.6
0.8
1.0
[C II] / PAH
νf_ν(70μm) / νf_ν(100μm)

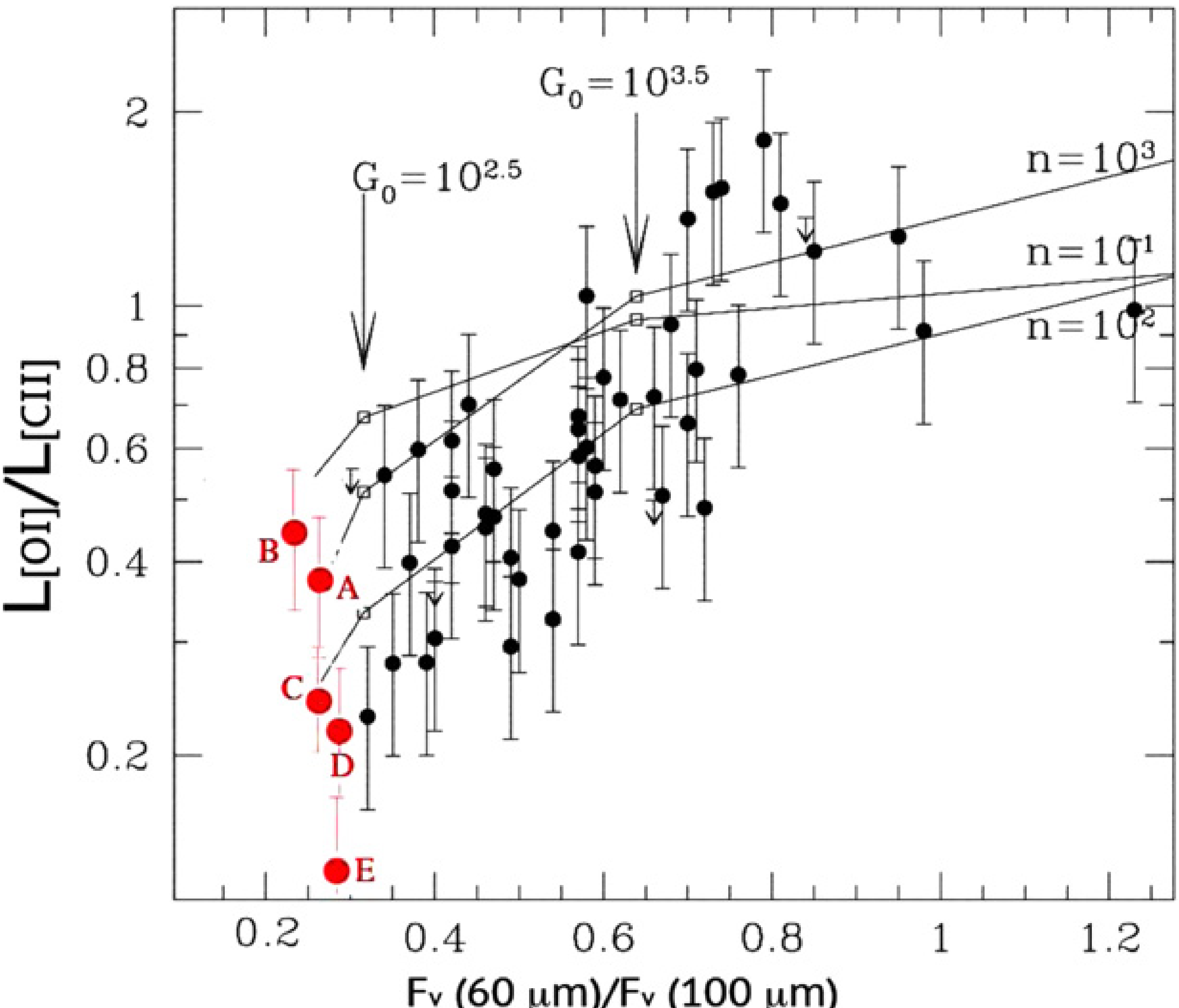

$G_0 = 10^{3.5}$
$G_0 = 10^{2.5}$
$n = 10^3$
$n = 10^1$
$n = 10^2$
B
A
C
D
E
2
1
0.8
0.6
0.4
0.2
0.2
0.4
0.6
0.8
1
1.2
$L_{[OI]}/L_{[CII]}$
F_ν (60 μm)/F_ν (100 μm)

1. Appleton et al. 2013, ApJ, 777, 66

Shock-enhanced C^+ Emission and the Detection of H_2O from the Stephan's Quintet Group-wide Shock Using Herschel

銀河相互作用によるショック領域で[CII]が明るくなることがわかった

2. Brisbin et al. 2014, arXiv:1411.1332

Strong C+ emission in galaxies at z~1-2: Evidence for cold flow accretion powered star formation in the early Universe

high-z ULIRGの1-10kpcにひろがった[CII]輝線領域（星形成起源）はインフローの証拠？

[CII]158um (CSO/ZEUS)

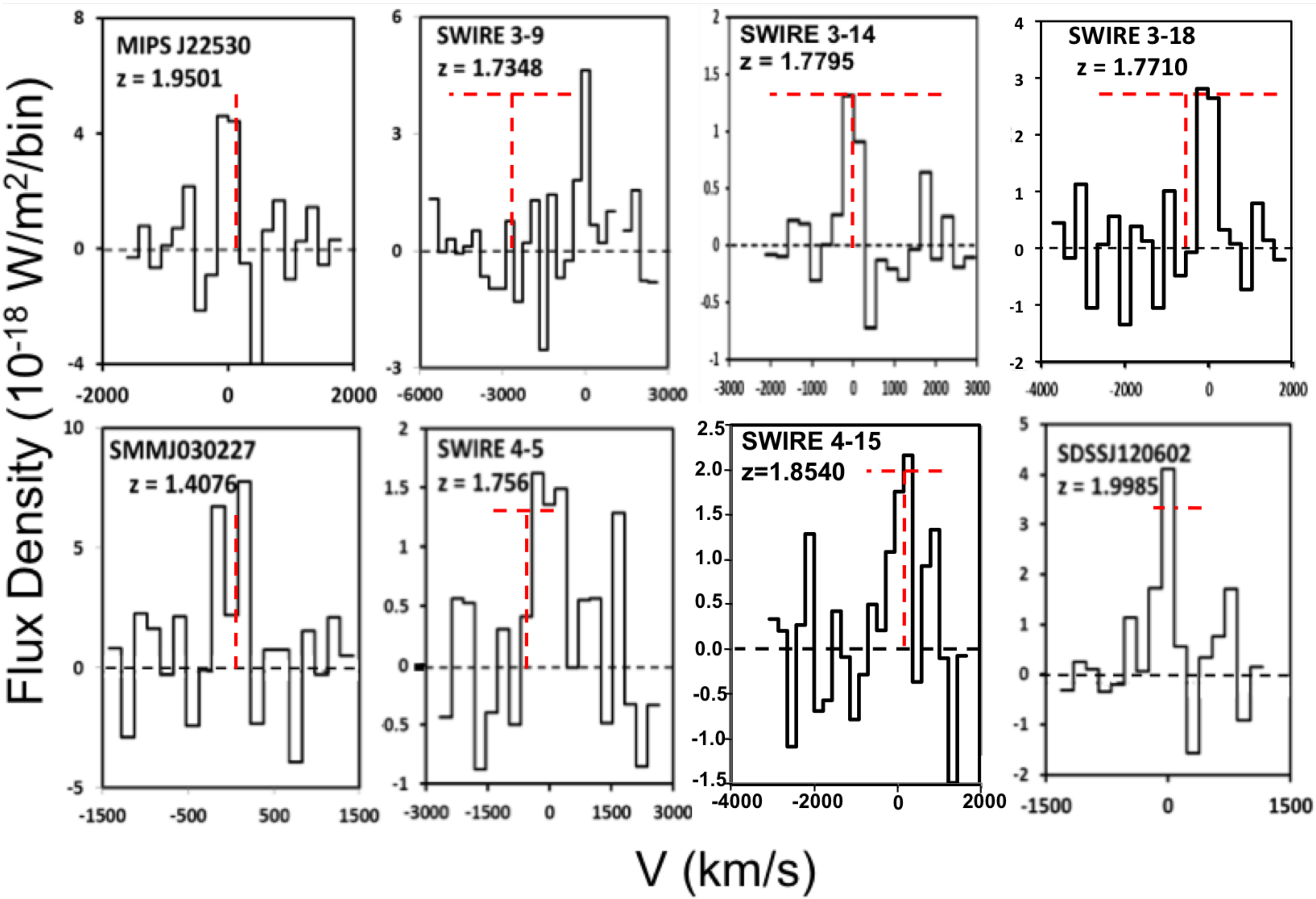

[OI]63um (Herschel/PACS)

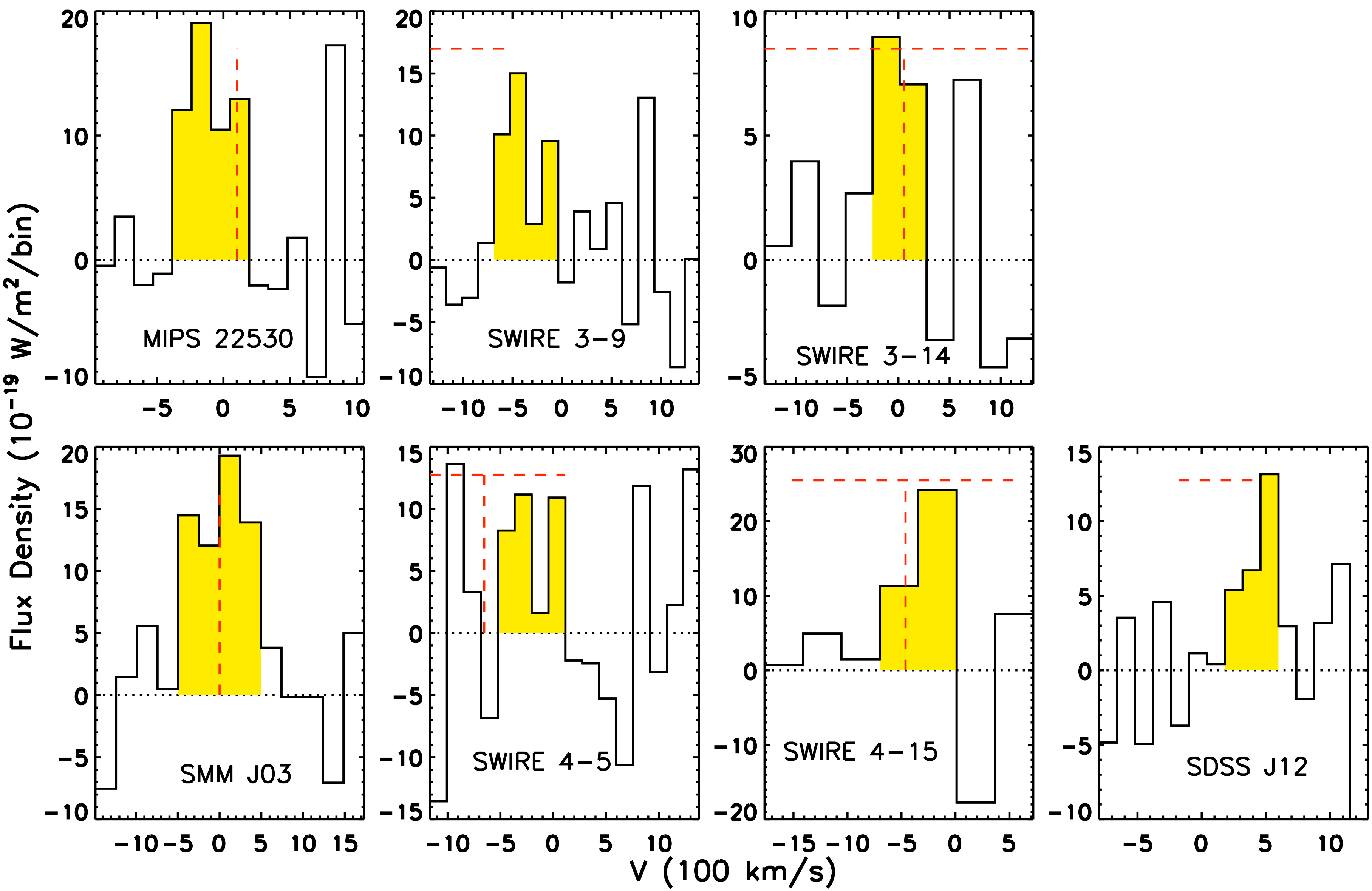

IR SED (MIPS/PACS/SPIRE)

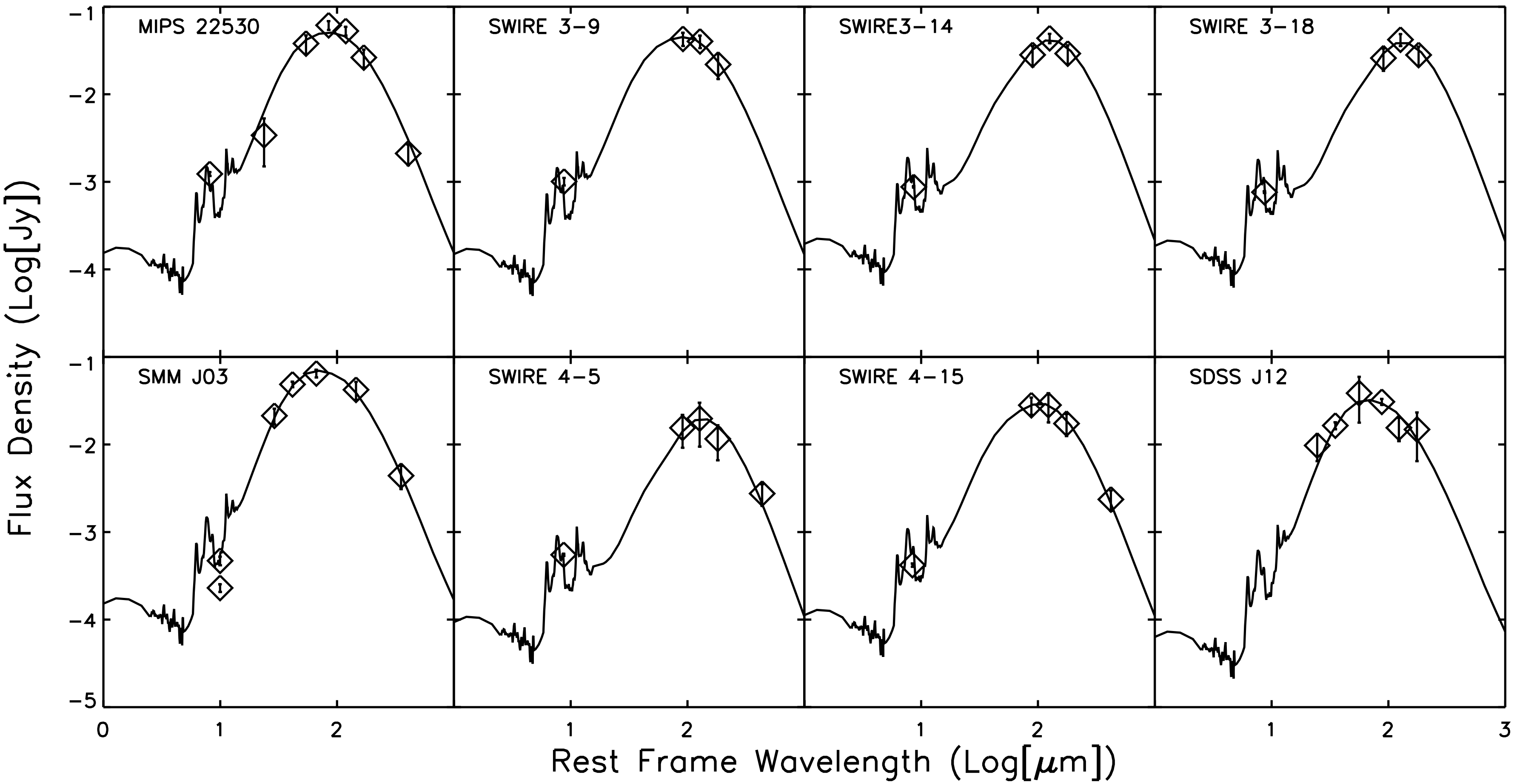

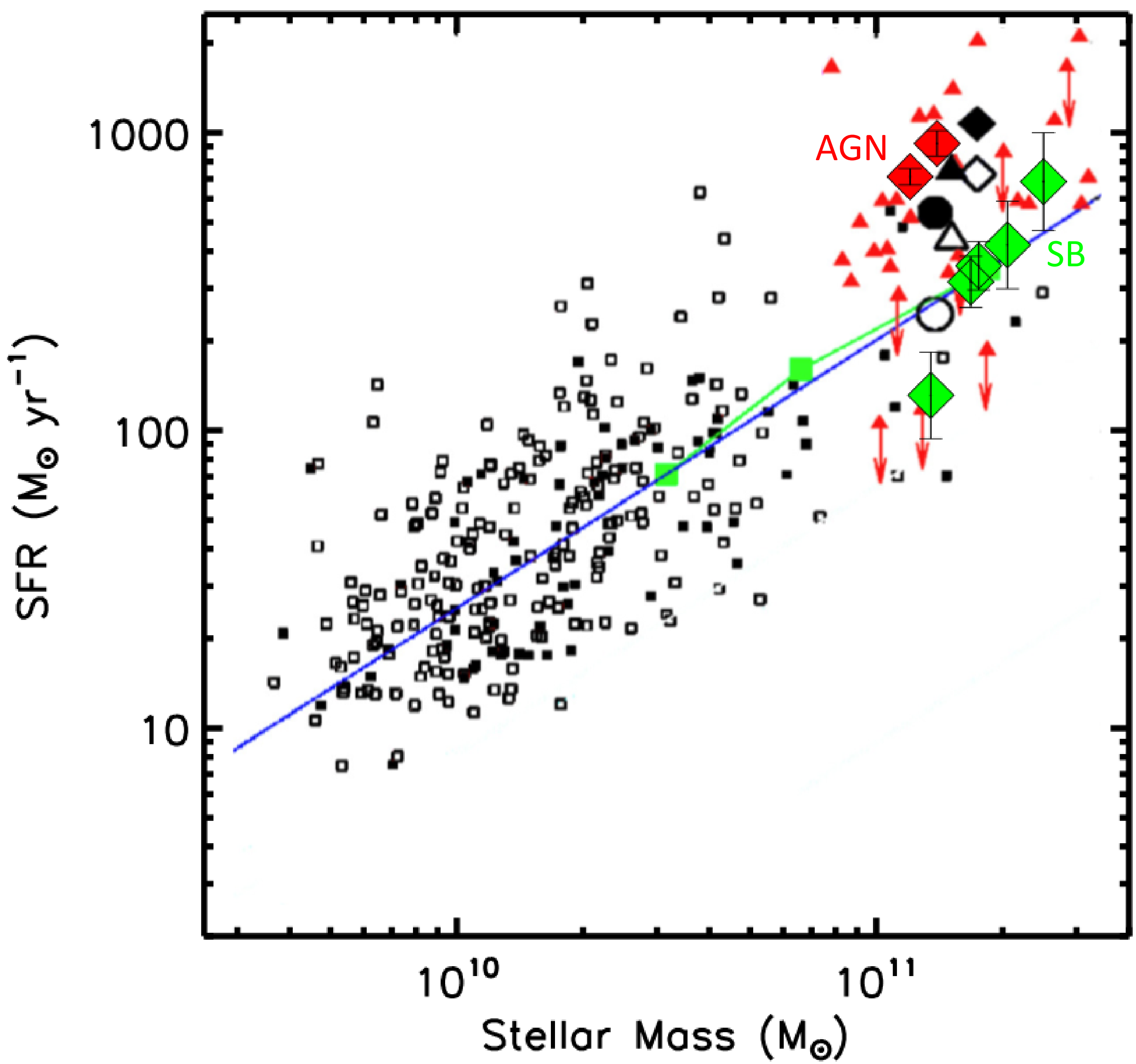

1000
100
10
SFR (M⊙ yr⁻¹)
10¹⁰
10¹¹
Stellar Mass (M⊙)
AGN
SB

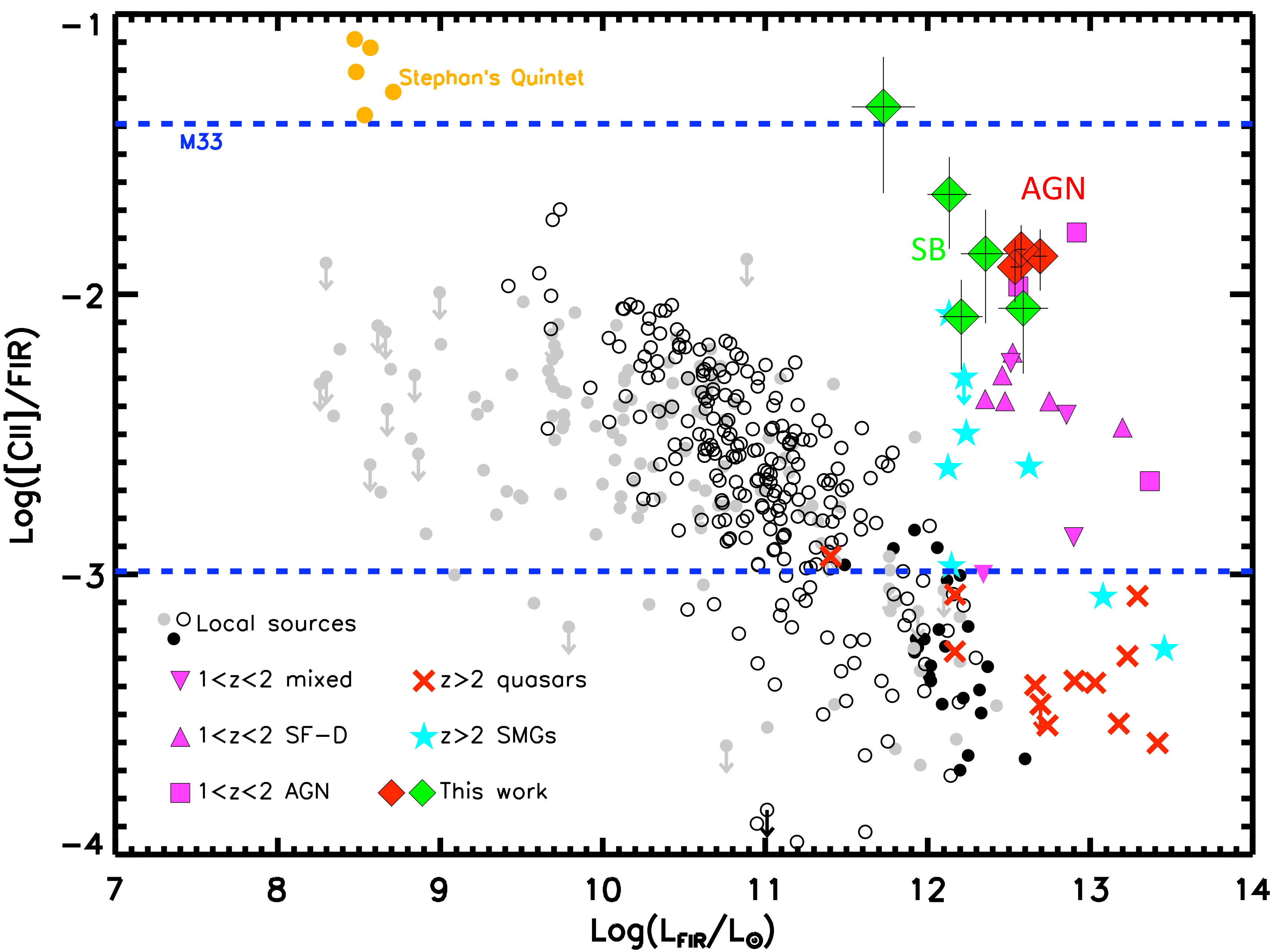

Stephan's Quintet
M33
AGN
SB
Local sources
1<z<2 mixed
z>2 quasars
1<z<2 SF-D
z>2 SMGs
1<z<2 AGN
This work
Log([CII]/FIR)
Log(LFIR/L⊙)
-1
-2
-3
-4
7
8
9
10
11
12
13
14

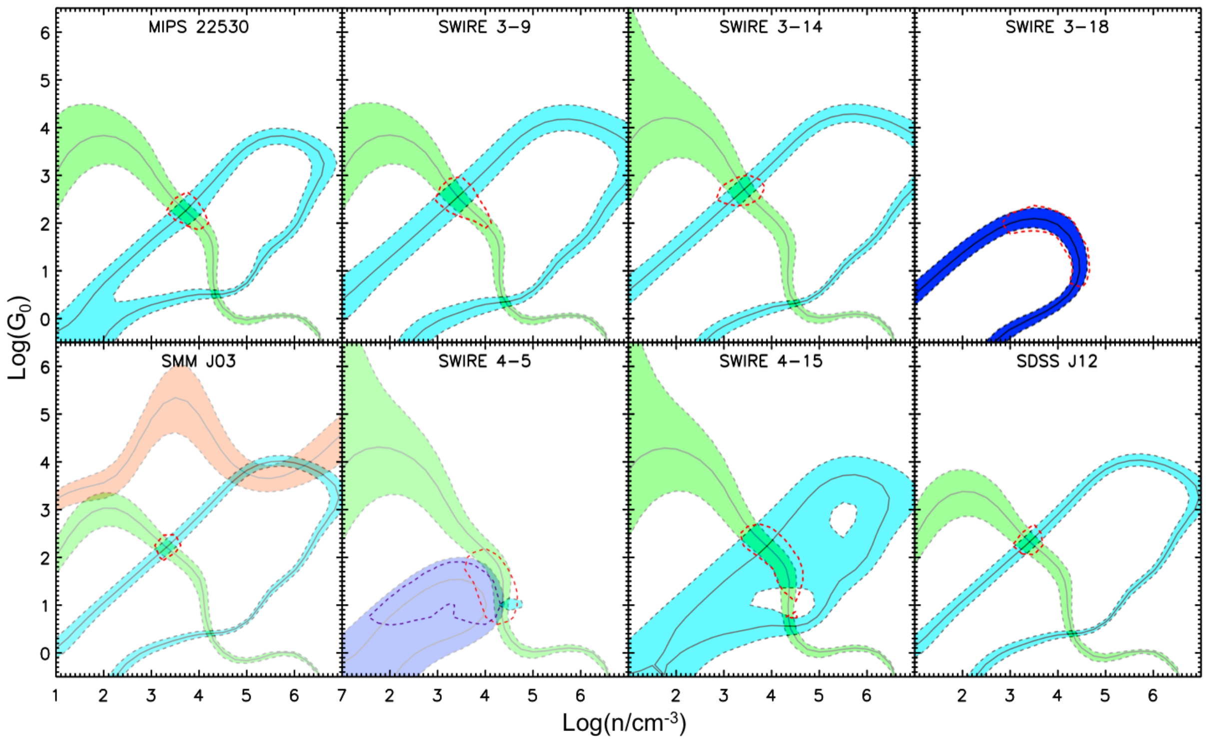

$$G_0 = F_{FUV}/1.6\times10^{-6}\ \mathrm{W\ m^{-2}}$$
$$G_0 \propto \lambda L_{IR}/D^3$$
$$(D/\mathrm{pc})^3 \sim 0.96\ (L_{FIR}/L_\odot)/G_0$$

Source	PDR parameters		
	log(n cm^3)	log(G$_0$)	size (kpc)
MIPS 22530	$3.75^{+0.25}_{-0.25}$	$2.25^{+0.25}_{-0.25}$	2.9-9.1
SWIRE 3-9	$3.5^{+0.5}_{-0.5}$	$2.5^{+0.25}_{-0.25}$	2.2-6.3
SWIRE 3-14	$3.5^{+0.25}_{-0.5}$	$2.75^{+0.25}_{-0.25}$	1.4-3.0
SWIRE 3-18	3-5	$2.0^{+0.25}_{-0.5}$	2.3-6.5
SMM J03	$3.25^{+0.25}_{-0.25}$	$2.25^{+0.25}_{-0.25}$	2.6-8.0
SWIRE 4-5	$4.25^{+0.25}_{-0.5}$	$1.25^{+0.5}_{-0.5}$	3.1-10.0
SWIRE 4-15	$4.25^{+0.25}_{-0.5}$	$2.25^{+0.25}_{-0.75}$	2.3-6.4
SDSS J12	$3.5^{+0.25}_{-0.25}$	$2.25^{+0.25}_{-0.25}$	2.6-7.6

green [OI]/[CII], cyan ([OI]+[CII])/IR, blue [CII]/IR, orange [OI]/CO(3→2)

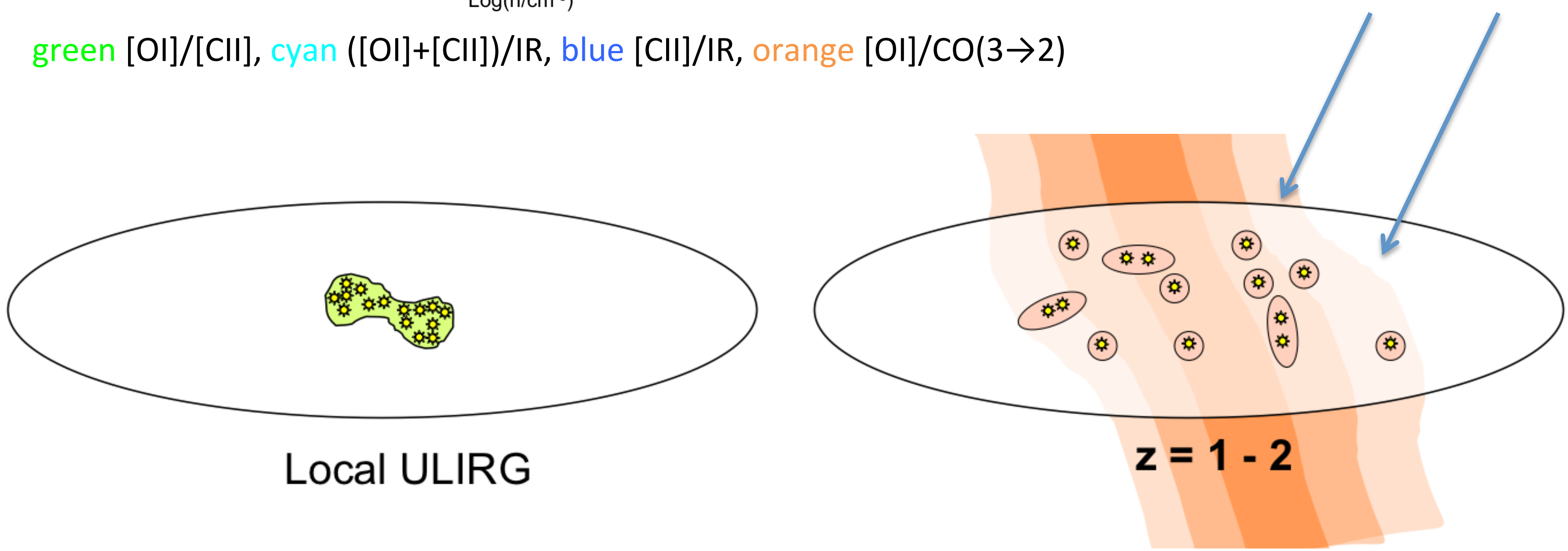

2. Brisbin et al. 2014, arXiv:1411.1332

Strong C+ emission in galaxies at z~1-2: Evidence for cold flow accretion powered star formation in the early Universe

high-z ULIRGの1-10kpcにひろがった[CII]輝線領域（星形成起源）はインフローの証拠？

3. Kreckel et al. 2014, ApJ, 790, 26

A Far-IR View of the Starburst-driven Superwind in NGC 2146

空間分解した[CII]速度分散マップからアウトフローが同定出来る

NGC2146

L_{IR}=1.2e11 Lsun (LIRG)
M_*=2e10 Msun
SFR=8 Msun/yr

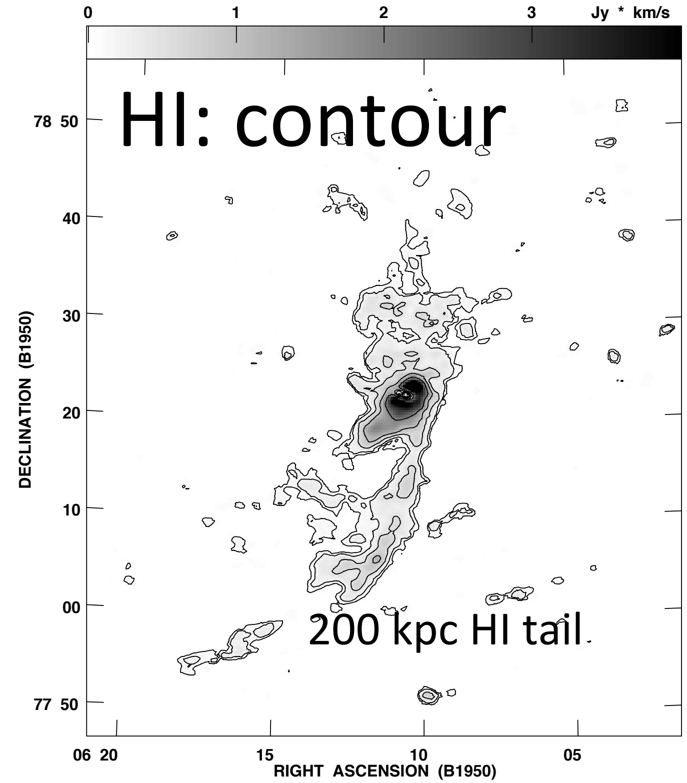

Taramopoulos+01

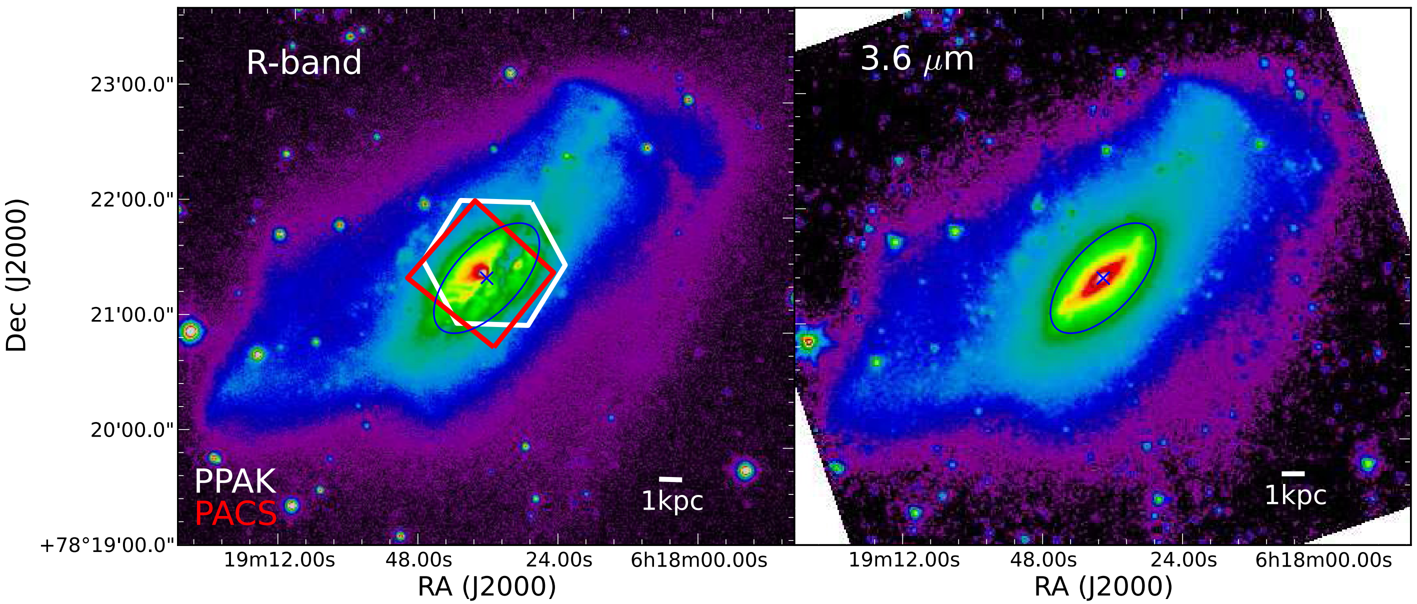

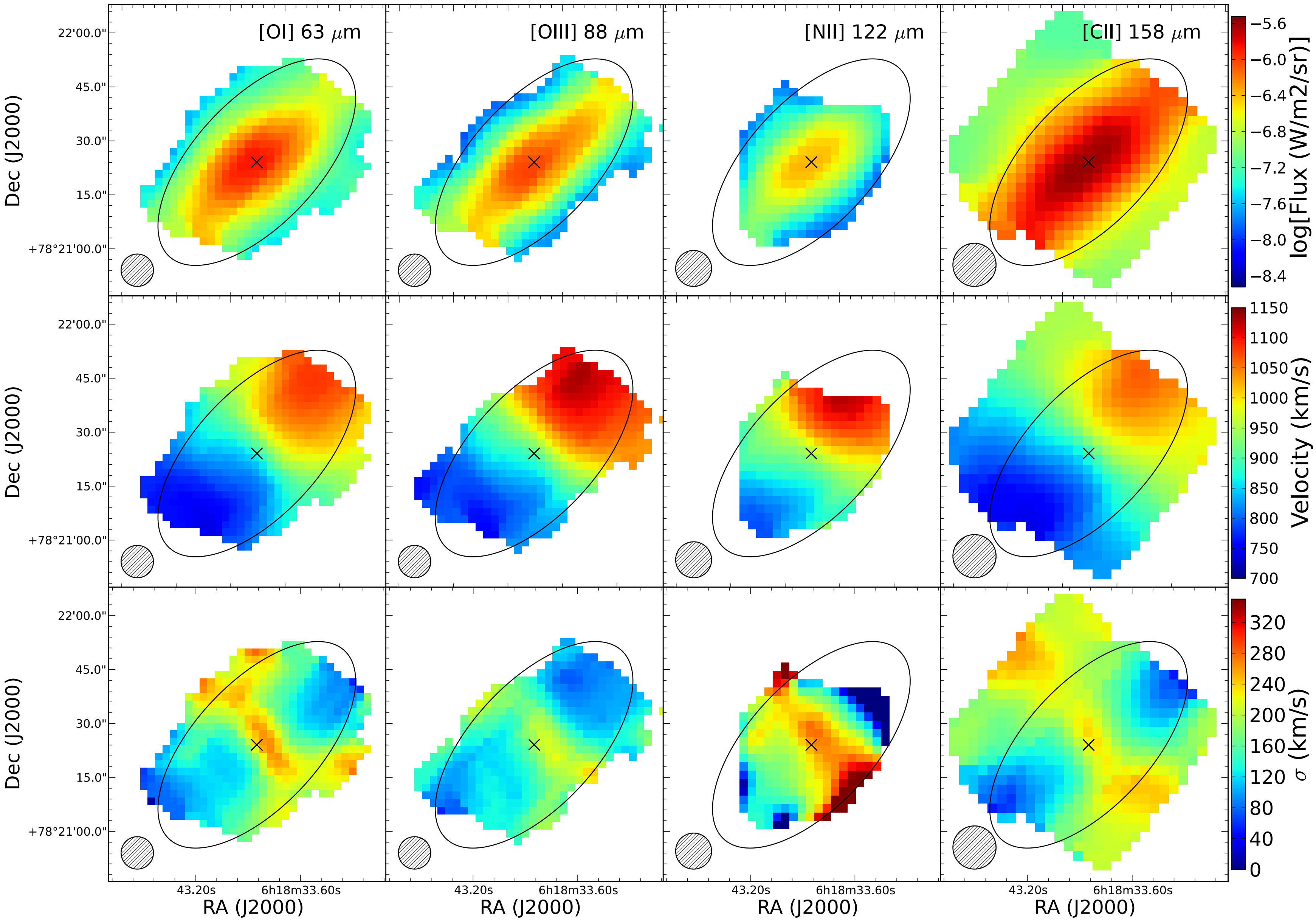

Figure 2. PACS spectroscopy line maps of (left to right) [O I] 63 μm, [O III] 88 μm, [N II] 122 μm, and [C II] 158 μm of the intensity (top), velocity (middle), and deconvolved velocity dispersion (bottom). The ellipse and center match those shown in Figure 1. All lines are masked in regions where the signal to noise is less than five. Uncertainties in the velocity dispersion are ~5% in the regions above and below the disk, and are much lower (<1%) within the disk. [N II] has velocity dispersion peaking at ~450 km s^{-1}. The point-spread function for each map is indicated in the lower left corner, and the 6 kpc ellipse shown for reference.

(A color version of this figure is available in the online journal.)

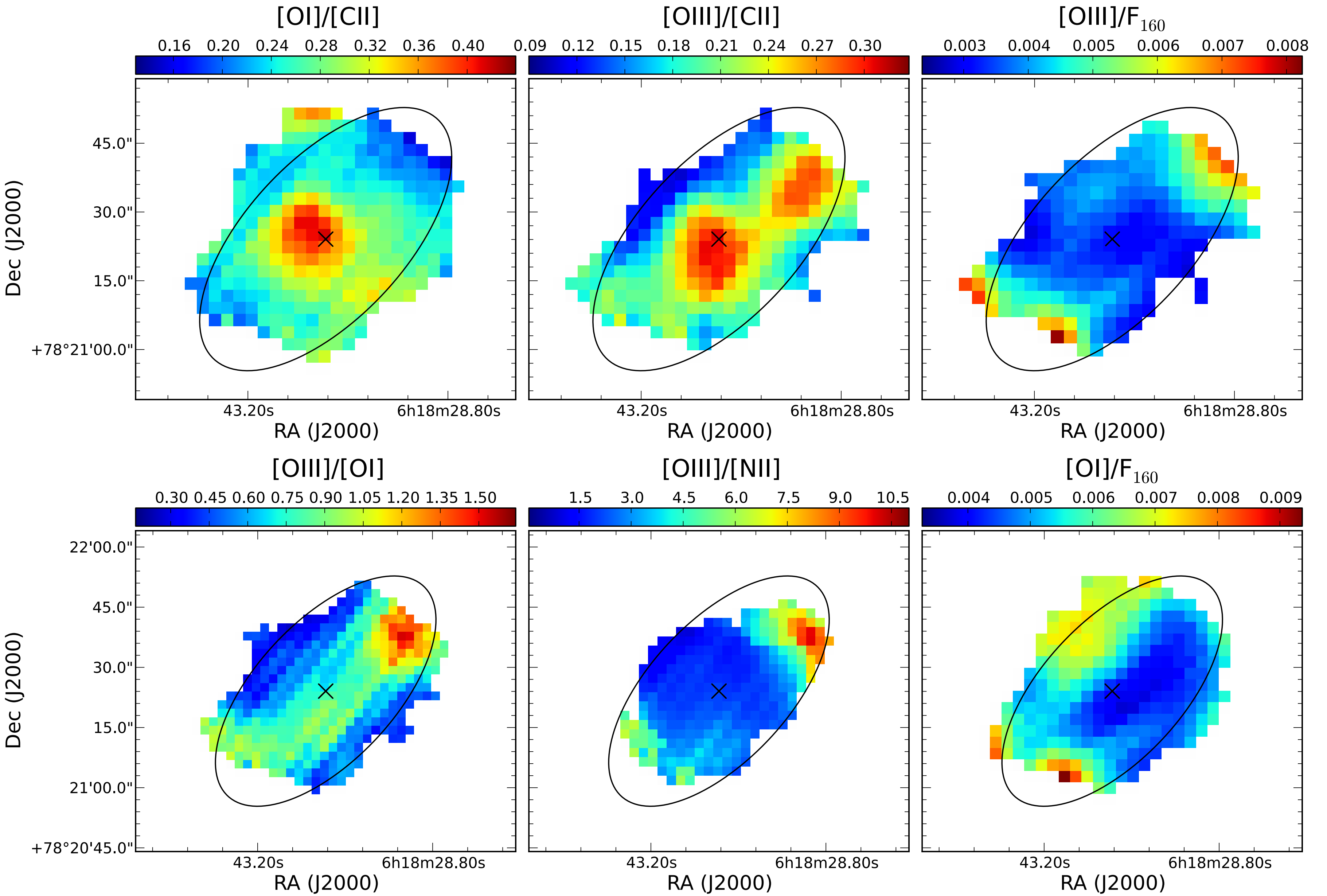

Figure 8. Line ratios of the far-IR fine-structure lines. The [O III]/[C II] and [O III]/[O I] ratios are consistent with star formation within the disk. The [O I]/[C II] ratio shows a different morphology, with a bright nucleus and a structure of high [O I]/[C II] that lies perpendicular to the disk, tracing the outflow. Uncertainties are typically 5%. The stellar disk and kinematic center (black) are marked for reference.

(A color version of this figure is available in the online journal.)

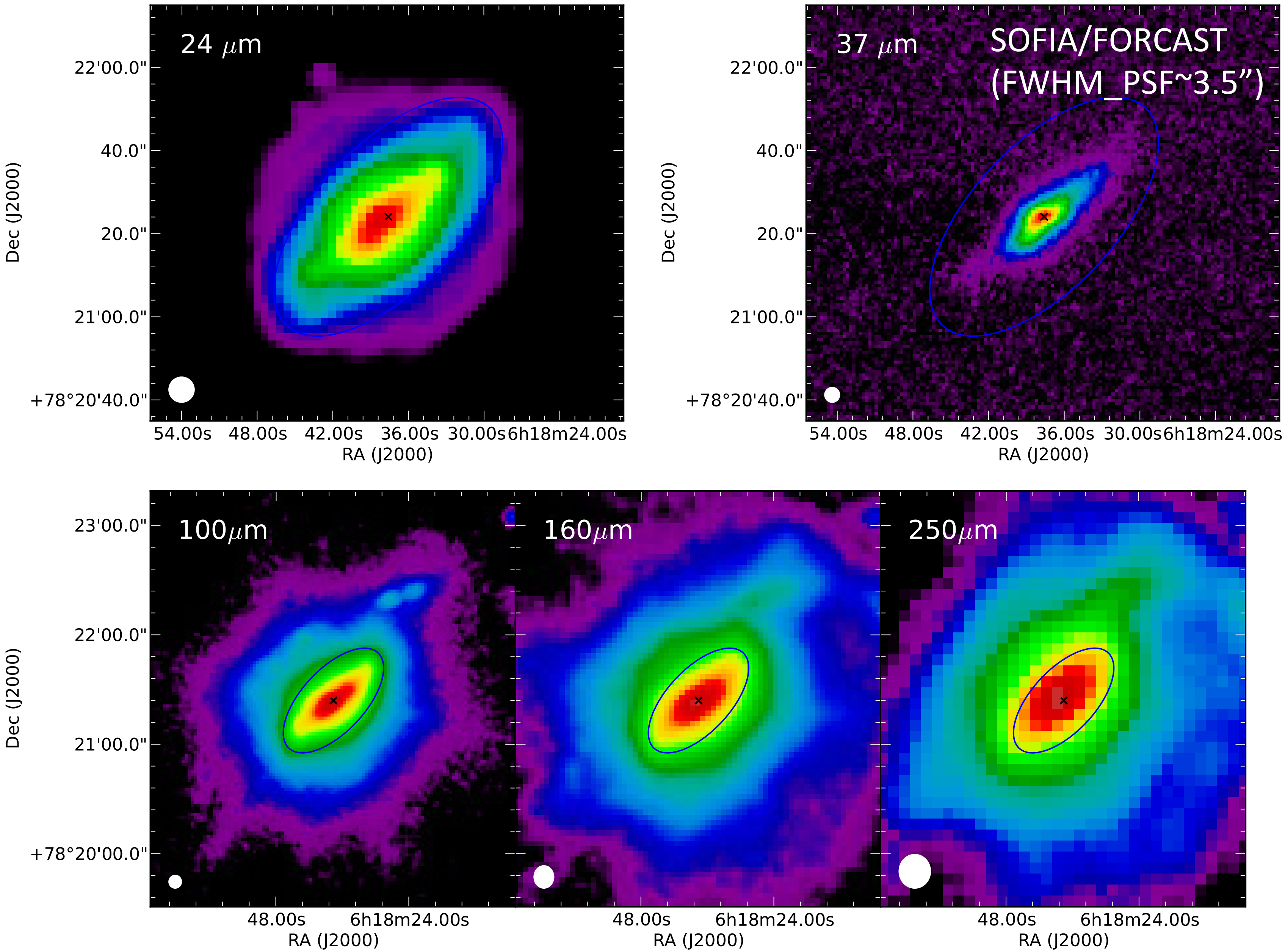

Figure 9. Dust emission in NGC 2146. Warm dust is traced by the *Spitzer* MIPS 24 μm emission (top left) and SOFIA FORCAST 37 μm emission (top right). Cold dust is traced by the *Herschel* PACS 100 μm (bottom left), 160 μm (bottom center), and SPIRE 250 μm (bottom right) emission. The emission generally follows the disk of the galaxy, with extended features that trace the optical spiral arms seen extending beyond the field of view of our line maps. Hexagonal features in the PACS images at low flux levels are due to the instrumental point-spread function. The stellar disk (blue oval) and kinematic center (cross) is marked for reference and is the same in all figures.

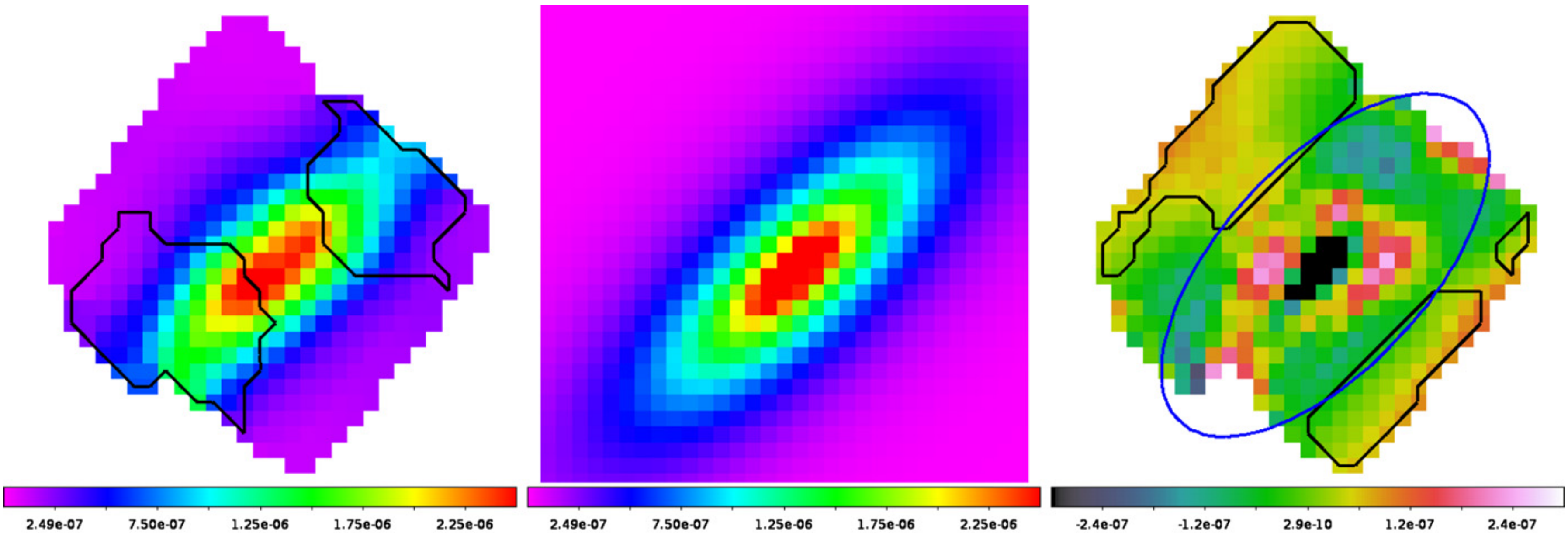

Figure 10. To identify the amount of [C II] emission in the outflow attributable to the outflow itself, we model the [C II] intensity distribution (left) using only those regions with low velocity dispersion (outlined in black) with a two-dimensional exponential disk (center). The residual from this fit (right) show an excess in the regions above and below the disk (in blue) that correspond to the regions with increased velocity dispersion (in black). From this we calculate an atomic gas outflow mass of $7.4 \times 10^8\ M_\odot$. If we assume that all [C II] emission in regions of high velocity dispersion is due to the outflow (with no disk component), we calculate an atomic gas mass of $3.9 \times 10^9\ M_\odot$.

$M_{\rm atomic,outflow}$~1e9 Msun

$$\frac{M_{\rm atomic}}{M_\odot} = 0.77\left(\frac{0.7 L_{[\rm C\,II]}}{L_\odot}\right)\left(\frac{1.4\times10^{-4}}{X_{C^+}}\right) \times \frac{1 + 2e^{-91K/T} + n_{\rm crit}/n}{2e^{-91K/T}}, \qquad (1)$$

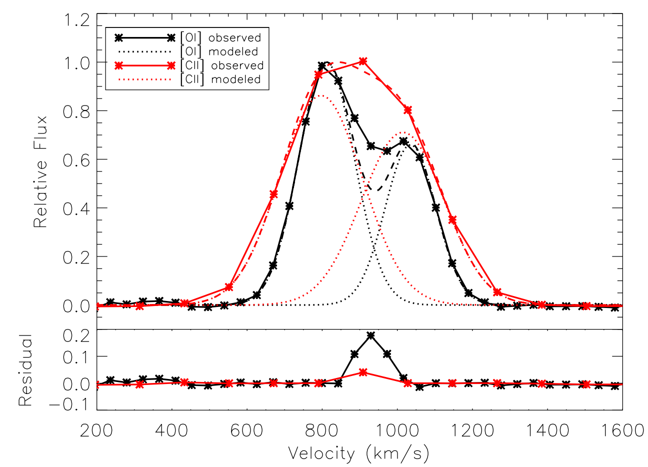

積分したスペクトルではアウトフロー成分を取り出すことはできなかった！

3. Kreckel et al. 2014, ApJ, 790, 26

A Far-IR View of the Starburst-driven Superwind in NGC 2146

空間分解した[CII]速度分散マップからアウトフローが同定出来る

まとめ

- ひろがった[CII]輝線で銀河相互作用によるショック領域をトレースできる
- 空間分解できなくても、[CII]輝線領域のサイズが求められる(大きなサイズはインフローを示唆？)
- 空間分解できれば[CII]速度分散マップからアウトフローが同定(diskと分離)出来る(~1kpc、0.1-0.2"@z=1-3が必要)